JOURNAL OF VIROLOGY, Jan. 2006, p. 426–439 Vol. 80, No. 1
0022-538X/06/$08.00+0 doi:10.1128/JVI.80.1.426–439.2006

Liver Transduction with Recombinant Adeno-Associated Virus Is Primarily Restricted by Capsid Serotype Not Vector Genotype

Dirk Grimm, Kusum Pandey, Hiroyuki Nakai,† Theresa A. Storm, and Mark A. Kay*

Departments of Pediatrics and Genetics, School of Medicine, Stanford University, 300 Pasteur Drive, Stanford, California 94305

Received 14 August 2005/Accepted 8 October 2005

We and others have recently reported highly efficient liver gene transfer with adeno-associated virus 8 (AAV-8) pseudotypes, i.e., AAV-2 genomes packaged into AAV-8 capsids. Here we studied whether liver transduction could be further enhanced by using viral DNA packaging sequences (inverted terminal repeats [ITRs]) derived from AAV genotypes other than 2. To this end, we generated two sets of vector constructs carrying expression cassettes embedding a *gfp* gene or the human factor IX (*hfIX*) gene flanked by ITRs from AAV genotypes 1 through 6. Initial in vitro analyses of *gfp* vector DNA replication, encapsidation, and cell transduction revealed a surprisingly high degree of interchangeability among the six genotypes. For subsequent in vivo studies, we cross-packaged the six *hfIX* variants into AAV-8 and infused mice via the portal vein with doses of 5×10^{10} to 1.8×10^{12} particles. Notably, all vectors expressed comparably high plasma hFIX levels within a dose cohort over the following 6 months, concurrent with the finding of equivalent vector DNA copy numbers per cell. Partial hepatectomies resulted in ~80% drops of hFIX levels and vector DNA copy numbers in all groups, indicating genotype-independent persistence of predominantly episomal vector DNA. Southern blot analyses of total liver DNA in fact confirmed the presence of identical and mostly nonintegrated molecular vector forms for all genotypes. We conclude that, unlike serotypes, AAV genotypes are not critical for efficient hepatocyte transduction and can be freely substituted. This corroborates our current model for AAV vector persistence in the liver and provides useful information for the future design and application of recombinant AAV.

Gene transfer vectors based on the single-stranded DNA parvovirus AAV (adeno-associated virus) are enormously popular and powerful tools for in vivo delivery of small DNA expression cassettes. The list of human genes carried by such cassettes is growing steadily and spans a wealth of clinically relevant candidates expressing blood coagulation factors (28), the cystic fibrosis transmembrane conductance regulator (18), or dystrophin (32), among many others. Most recently, AAV vectors have begun to attract particular attention for delivery of short hairpin RNAs, and indeed, with a packaging capacity of 5 kb DNA and the promise to mediate safe and persistent gene transfer, they appear as bona fide tools for in vivo RNA interference applications (27).

A major reason for AAV's broad and growing appeal is the feasibility to pseudotype the recombinant viral DNA, i.e., to generate particles in which the vector DNA (genotype) and the viral capsid (serotype) differ in their AAV origins (23). The resulting hybrid particles are typically characterized by unique receptor tropisms and are distinctly recognized by the host immune system, as determined by the capsid. Thus, the pseudotyping approach has dramatically extended the array of cells and tissues susceptible to AAV gene transfer and relieved some of the concerns associated with the abundance of neutralizing antibodies against the AAV prototype, AAV-2, in the human population (24).

* Corresponding author. Mailing address: Departments of Pediatrics and Genetics, School of Medicine, Stanford University, Room G305, 300 Pasteur Drive, Stanford, CA 94305. Phone: (650) 498-6531. Fax: (650) 498-6540. E-mail: markay@stanford.edu.

† Present address: Departments of Molecular Genetics and Biochemistry, School of Medicine, University of Pittsburgh, Pittsburgh, PA 15261.

Fortunately, the list of known AAV serotypes is expanding progressively and currently spans more than 100 isolates, including AAV-1 through -11, as well as a plethora of partially cloned human and primate variants, with genome homologies between 55 and 85% (4, 8, 9, 19–21, 36, 55, 59, 68). To date, 13 of these serotypes have been vectorized (AAV-1 to -11, avian and bovine AAVs), with AAV-8 perhaps being the most remarkable candidate. This variant has recently engendered significant interest for gene transfer to the liver and several other tissues, where it results in extremely rapid and efficient transduction due to inherently fast kinetics of uncoating the vector DNA (21, 38, 63, 64).

Surprisingly, despite the extensive progress achieved by modifying the viral serotype, attempts to improve AAV gene transfer by varying the vector genotype have been rarely reported to date. This is particularly remarkable considering the essential role in the AAV life cycle played by the components that determine the genotype, i.e., the inverted terminal repeats (ITRs) flanking the viral DNA (1, 3, 56, 61, 65, 66, 69) (see also Fig. 7). Briefly, during virus production, they serve as rescue signals mediating excision of the embedded genome from the vector plasmid, before initiating amplification of the rescued DNA, by assuming a hairpin shape and providing a free end for binding of cellular DNA polymerase. Subsequently, they trigger progeny DNA encapsidation by binding viral replication (Rep) proteins and mediating association with the capsid. Finally, during transduction, they play roles in the transformation of single-stranded input genomes into active double-stranded DNAs with further processing to episomal or integrated higher-molecular-weight forms, although their exact contribution is tissue specific and controversial (see Discussion). Notably, AAV-2 ITRs are also integral regulators of wild-type gene

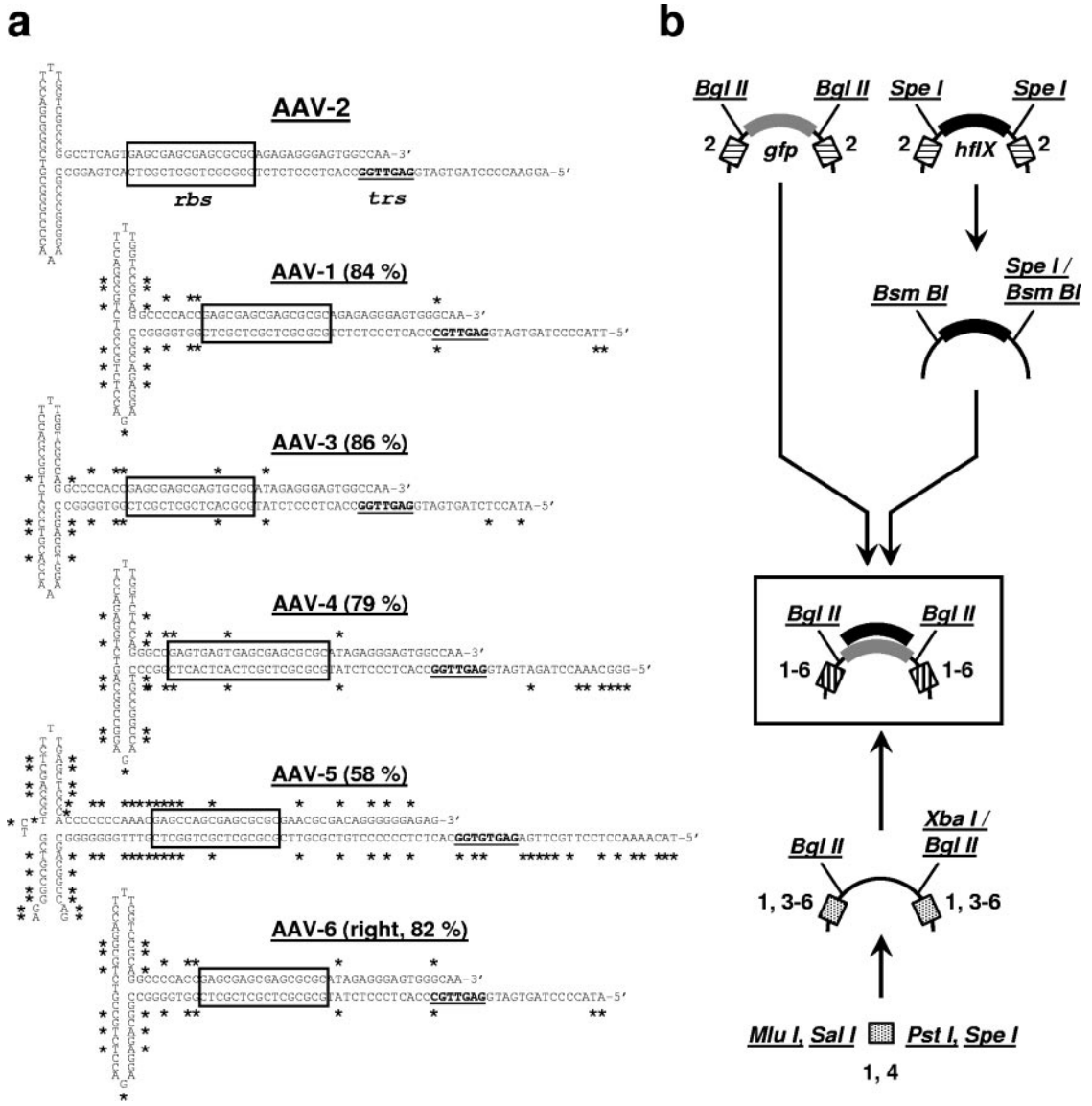

FIG. 1. Structures, sequences, and cloning of ITRs from AAV genotypes 1 to 6. (a) ITRs from AAV-1 through -6. Nucleotide sequences and structures were assembled from various previous publications (8, 9, 55, 68). Shown at the top is the AAV-2 prototype ITR, with the Rep protein binding site (*rbs*) and the terminal resolution site (*trs*) highlighted. Depicted below are the five alternative ITRs used here, with asterisks marking nucleotide differences compared to AAV-2 and values in parentheses indicating overall sequence homologies with AAV-2. Note that the right AAV-6 ITR is shown, while the left variant is identical to AAV-2 (55, 68). (b) Cloning of genotyped AAV vectors (scheme). The six AAV ITRs were derived from multiple sources (molecular clones or de novo synthesis) and cloned as detailed in Materials and Methods to yield plasmids in which they were flanking BglII or BamHI sites. This permitted the straightforward insertion of *gfp* or *hfIX* transgene expression cassettes as compatible fragments.

expression (30, 67), and vector studies likewise suggested an intrinsic weak promoter activity for these ITRs, along with the ability to bind regulatory cellular factors (5, 14).

The two elements within the AAV-2 prototype ITR mediating most of these functions, i.e., the sites for Rep protein binding (*rbs*) and terminal resolution (*trs*), are shown in Fig. 1a. With few exceptions (see below), these sites are largely conserved among all eight AAV isolates that have been fully cloned to date, namely, AAV-1 through -6, as well as avian (AAAV) and bovine (BAAV) AAVs. Likewise maintained is the capability of all single-stranded ITRs to assume a secondary hairpin structure despite variations in total length from 142 (AAAV) to 167 (AAV-5) nucleotides and DNA homologies as low as 55% (4, 24, 59) (AAV-5 and the rest).

Interestingly, a few of the known ITRs are also unique in some aspects, the best example being AAV-5. As discovered by Chiorini et al., the particular sequence and positioning of the *trs* element within the AAV-5 ITR (Fig. 1a) prevent nicking by Rep from a heterologous variant such as AAV-2 (7). We moreover recently found that among AAV-1 to -6, only AAV-5 Rep proteins are able to resolve the AAV-5 ITR and that, vice versa, AAV-5 Rep cannot nick ITRs from AAV-2, -3, or -6

(25). A drawback of this uniqueness is that the AAV-5 genotype is hard to pseudotype, which hampered analyses of the contribution of AAV-5 ITRs to vector function in the past and represented a hurdle we had to overcome in the present study (see Results). AAV-5 ITRs are also the only candidates other than AAV-2 for which an intrinsic promoter activity was reported, a property that could be exploited by flanking vector DNAs with AAV-5 ITRs, as was previously suggested (17, 52).

A second example of a unique ITR is AAV-4, which carries an extended *rbs* element containing five, instead of four, copies of the Rep-binding GMGY repeat. This sparked speculation that it might possess a higher binding affinity for Rep, to potentially affect genome replication, packaging, or persistence in the target cell (9). However, this remains hypothetical since vectors carrying AAV-4 ITRs were never made or tested.

A third remarkable genotype is AAV-6, which is a hybrid between AAV-1 and -2 and thus carries an ITR from each isolate (55, 68). To date, the consequences for the virus or vectors derived therefrom remain unknown. Interestingly, Halbert et al. found that vectors with AAV-2, -3, or -6 ITRs differed in transduction of cultured cells (29), but it remains uncertain whether their results will translate to animal models.

Intrigued by these previous findings and presumptions, we wanted to perform a thorough comparison of all ITRs whose sequences were known at the time of this work, i.e., AAV-1 to -6. Previously, we had begun to study ITRs from genotypes 2, 3, 5, and 6 but our analyses were restricted to cultured cells and in vivo vector performance was not tested (25). Here we report a more comprehensive study characterized by the addition of two further genotypes, AAV-1 and -4, allowing evaluation of a set of ITRs from six different AAVs, and the development of a novel hybrid helper plasmid, permitting efficient pseudotyping of the AAV-5 genotype with capsids from AAV-8. We present extensive data from the in vivo long-term (6 months) comparison (protein and DNA levels) of all six genotypes in whole animals (mice), following liver-directed vector DNA transfer with the AAV-8 capsid.

We believe that the novel tools and findings reported here will significantly further our understanding of the mechanism of liver transduction with recombinant AAV and will moreover have multiple levels of impact on future AAV vector design and production.

MATERIALS AND METHODS

Culture and infection of cell lines. Human HeLa and 293 embryonic kidney cells were maintained in Dulbecco modified Eagle medium (Gibco) containing 10% fetal calf serum, 2 mM L-glutamine, and 50 IU/ml each of penicillin and streptomycin at 37°C in 5% CO_2. For infection with Gfp-expressing AAV vector particles, HeLa cells were plated in 96-well dishes at a concentration of 10^4 cells in 100 μl per well. The next day, 10 μl virus suspension was added to the first well and then serially 10-fold diluted a total of seven times. Following a 2-day incubation, Gfp-expressing cells were counted under a fluorescence microscope and titers of infectious particles calculated, taking into account dilution factors and the starting volume (10 μl; see above).

Cloning of AAV genotype vectors and hybrid AAV-5/-8 helpers. The AAV-2-based vector plasmid pTRUFΔ was previously reported by our group (26) and is based on pTRUF5, which was initially kindly provided by N. Muzyczka. AAV vector plasmids carrying the ITRs from genotype 3 or 6 were kindly provided by D. Russell. In all three constructs, a BglII site is present between each ITR and the original insert, allowing easy replacement of the entire cassette with appropriately digested fragments (see below). The AAV-5-based vector construct p7D05 was kindly provided by J. Chiorini and R. Kotin (60) and engineered by inserting fragments into the BglII and XbaI sites located adjacent to the left or right AAV-5 ITR, respectively.

Vector plasmids containing the ITRs from AAV-1 or -4 were not available at the time of our study and were thus de novo generated by using the commercially obtainable plasmid pDNR-1r (BD Clontech, Palo Alto, CA) as the basis for cloning. The AAV-1 and -4 ITRs themselves were synthesized based on published sequences (9, 68) by GeneArt (Regensburg, Germany).

For easy cloning of the AAV-1 and -4 ITRs, they were synthesized together with flanking sequences comprising MluI and SalI sites (5′-ACGCGTGTCGA C-3′; left ITR) or PstI and SpeI sites (5′-CTGCAGACTAGT-3′; right ITR). The ITRs were provided in the plasmid pCR4Blunt-TOPO (Invitrogen, Carlsbad, CA).

In a first step, we eliminated the NheI, BglII, and MluI restriction sites present in pDNR-1r by linearizing with NheI and MluI and then inserting annealed oligonucleotides 5′-CTAGGCTTCGATCTGCTCTAGGCCACCTG-3′ and 5′-CGCGCAGGTGGCCTAGAGCAGATCGAAGC-3′. Subsequently, after linearization of the resulting construct with XhoI and SpeI, annealed primers 5′-TCGAGGCTAGCTCCAGCTATCACGCGT-3′ and 5′-CTAGACGCG TGATAGCTGGAGCTAGCC-3′ were inserted to introduce NheI and MluI restriction sites (underlined) into the multiple cloning site, yielding plasmid pDNR-2O. One copy of the AAV-1 or -4 ITR was then cloned as a SalI/PstI fragment into the appropriately digested pDNR-2O construct, followed by insertion of the *gfp* or *hfIX* expression cassettes as BglII or BsmBI fragments (see below) by using the central BamHI site in pDNR-2O for linearization. In a final step, a second ITR copy was cloned into the resulting four constructs, this time by using the flanking MluI and SpeI sites for isolation from the pCR4Blunt-TOPO backbone and MluI together with NheI (*gfp*) or SpeI (*hfIX*) sites in the vector plasmids for insertion.

Plasmid pBSIICM (33) was used to isolate a human coagulation factor IX expression cassette comprising a liver-specific promoter (the apolipoprotein E hepatic locus control region-human a1-antitrypsin gene promoter), the *hfIX* minigene (containing a 1.4-kb fragment of the first intron from the *hfIX* gene), and the bovine growth hormone poly(A) signal. To allow subcloning of the entire *hfIX* cassette into the six genotyped vectors with ease, the following strategy was used. First, a short linker containing XbaI and SpeI sites, flanked by two BsmBI sites, was introduced into XbaI/EcoRI-linearized pBlueScriptII (Stratagene, La Jolla, CA) by using annealed oligonucleotides 5′-CTAGCGTCTCCGATCC*TC TAGA*AGCCATCGACTAGTCGTCTCGGATCG-3′ and 5′-AATTCGATCC GAGACGACTAGTCGATGGCTTCTAGAGGATCGGAGACG-3′ (BsmBI sites are underlined, and XbaI and SpeI sites are in italics). Subsequently, the entire *hfIX* cassette was isolated from pBSIICM by digestion with SpeI and subcloned into XbaI/SpeI-linearized, linker-containing pBlueScriptII. From there, it was released by digestion with BsmBI, leaving BglII-compatible overhangs at both ends. The *hfIX* cassette was inserted as a BsmBI fragment into BglII-linearized AAV-2, -3, and -6 vector plasmids or BamHI-cut AAV-1 and -4 constructs. For cloning into the Bg1II/XbaI-linearized AAV-5 vector plasmid, the *hfIX* insert was isolated by digestion with BsmBI and SpeI.

A cytomegalovirus (CMV) promoter-driven *gfp* gene was isolated from plasmid pTRUF5Δ by digestion with BglII and inserted into the six genotype vector plasmids following their linearization with BglII (AAV-2, -3, -5, and -6) or BamHI (AAV-1 and -4).

Hybrid helpers expressing AAV-5 Rep together with AAV-8 capsid proteins were constructed by replacing the AAV-2 *rep* gene in p5E18V2/8 (21) with a set of eight PCR products spanning the entire AAV-5 *rep* gene. For all PCRs, the forward primer 5′-GCAGAGGTCGACGCGTATGAGTTCTCGCGAGAC TTCCG-3′ was used, together with each of the following reverse primers (the last letters in the primer names correspond to those in Fig. 3a): R5A, 5′-CCTGAG TACGTACTTTATTTACTGTTCTTTATTGGCATCG-3′; R5B, 5′-CCTGAG TACGTACTCGCTTTATTTACTGTTCTTTATTGGC-3′; R5C, 5′-CCTGAG TACGTAACTCGCTTTATTTACTGTTCTTTATTGG-3′; R5D, 5′-CCTGAG TACGTATACTCGCTTTATTTACTGTTCTTTATTGG-3′; R5E, 5′-CCT GAGTACGTACTACTCGCTTTATTTACTGTTCTTTATTG-3′; R5F, 5′-CCT GAGTACGTAACTACTCGCTTTATTTACTGTTCTTTATTG-3′; R5G, 5′-CCTGAGTACGTAGACTACTCGCTTTATTTACTGTTCTTTATTG-3′; R5H, 5′-CCTGAGTACGTATGACTACTCGCTTTATTTACTGTTCTTTATTG-3′. Plasmid pRC5 (25) was used as the template for all reactions. Underlined sequences denote SalI or SnaBI sites in the forward or all reverse primers, respectively, which were used for directional subcloning of the various PCR products into SalI/SnaBI-linearized p5E18V2/8.

AAV vector particle production and titration. Analytical small-scale AAV productions were carried out in 6-cm culture dishes by using ~10^6 293 cells per dish and a total of 6 μg plasmid DNA. This total amount consisted of a 1:1:1 molar ratio mixture of genotyped *gfp*-encoding AAV vector plasmid, AAV-1-

through -6-specific AAV helper plasmid (pRC1 through pRC6) (25), and adenoviral helper (25). Transfections were carried out by using a standard calcium phosphate-based protocol (23), and cells were incubated for 2 days before crude AAV particle extracts were prepared by subjecting the cells to three consecutive freeze-thaw cycles.

For preparative large-scale productions, a previously published procedure was employed by using batches of 50 T225 (Corning Inc., Corning, NY) flasks per virus preparation (23). The cells were transfected with a total of 75 μg plasmid DNA per flask, consisting of an equimolar mixture of genotyped *hfIX*-encoding vector plasmid, AAV-8 pseudotyping helper plasmid (p5E18V2/8 for packaging of genotypes 1 to 4 and 6 or AAV-5/-8 clone H for genotype 5), and adenoviral helper. All six genotyped AAV-8 preparations were processed identically by using two rounds of cesium chloride (CsCl) gradient centrifugation for purification, ultrafiltration-diafiltration (Amersham, Piscataway, NJ) for CsCl removal and particle concentration, and dot blot titration for quantification (23). Final viral preparations were kept frozen at −80°C in phosphate-buffered saline (PBS) containing 5% sorbitol.

Animal studies. Six- to eight-week-old female C57BL/6 mice were obtained from Jackson Laboratory (Bar Harbor, ME). All animal procedures were done according to the guidelines of animal care at Stanford University. Portal vein infusion of AAV suspensions diluted in 1× PBS and two-thirds partial hepatectomies were performed as earlier described (45). Blood samples were collected from the retro-orbital plexus. Measurements of plasma human FIX levels were carried out by an hFIX-specific enzyme-linked immunosorbent assay (ELISA) procedure as reported previously (45).

Western and Southern blot analyses. AAV proteins were extracted from transfected cells and detected by Western blot analysis as previously described (25). As the primary antibody for AAV Rep or VP detection, monoclonal antibody 303.9 or B1 was used (25), respectively, at a 1:10 dilution in 6% nonfat milk. Secondary anti-mouse immunoglobulin G coupled with horseradish peroxidase (Amersham) was diluted 1:4,000 in nonfat milk to allow ECL detection (Amersham).

Extrachromosomally replicated AAV vector DNA was extracted from transfected 293 cells following a modified Hirt procedure as described in detail earlier (25). Samples were analyzed by Southern blotting with a standard protocol for transfer and a radioactively labeled CMV-specific probe for detection of all six *gfp*-encoding genotyped vectors.

For extraction of total genomic liver DNA from AAV-transduced mice, a previously reported phenol-free method was used (6). To analyze vector DNA copy numbers or molecular forms, 10 μg of each DNA sample was digested with the enzymes indicated in Results or in the figure legends, typically with 40 to 100 U of enzyme in an overnight reaction to guarantee complete restriction. Samples were then separated on 1% agarose gels and transferred to positively charged nylon membranes (Amersham) by a standard protocol. For quantification of AAV vector copy numbers, a standard curve was prepared by adding specific amounts of *hfIX* AAV-2 vector plasmid to 10 μg of total liver DNA from a naive C57BL/6 mouse. Plasmid amounts were calculated to give the numbers of double-stranded vector genomes per diploid genomic equivalent shown in Fig. 5b. All DNAs were detected with a radioactively labeled full-length *hfIX* probe, and band intensities were quantified with a G710 Calibrated Imaging Densitometer (Bio-Rad, Hercules, CA) to determine the vector copy number in each sample.

RESULTS

Construction of AAV vectors with sequences from AAV genotypes 1 to 6. The aim of this work was to investigate whether and to what extent the genotype origin of AAV ITRs would affect the recombinant viral life cycle. To this end, we generated two series of AAV vector constructs carrying a *gfp* gene or the human blood coagulation factor IX (*hfIX*) gene flanked by ITRs from AAV genotypes 1 through 6. From here on, this process will be referred to as "genotyping," and we suggest the term "genotyped" AAV for recombinant particles carrying genotype-specific ITRs, in analogy to "pseudotyped."

The six AAV isolates were chosen because their complete DNA sequences were known at the time of this study and because this ITR set provided a high degree of genetic heterogeneity, with sequence homologies as low as 58% (AAV-5 and the rest, Fig. 1a). A particularly unique and interesting candidate was provided by AAV-6, which carries distinct ITRs derived from two alternative isolates (68) (AAV-1 and -2, Fig. 1a). Out of the six AAV ITRs, one (AAV-2) was already present as a molecular clone in our group and three others (AAV-3, -5, and -6) were kindly provided by R. Kotin and D. Russell. In addition, we chemically synthesized the two ITRs from AAV-1 and -4 based on published sequences (9, 68). A cloning strategy was then devised to yield plasmids in which all ITRs were flanking common restriction sites to allow the straightforward insertion of our transgene expression cassettes of interest (Fig. 1b).

Our first specific aim was to study whether a particular ITR genotype would provide the vector DNA with a replication or packaging advantage over the AAV-2 prototype and whether this required the expression of serotype-specific AAV proteins. Therefore, we cotransfected 293 cells with the six individual *gfp* constructs, together with each of six AAV helper plasmids expressing replication (Rep) and capsid (VP) proteins of AAV-1 through -6. A third plasmid added to all reaction mixtures expressed helper functions from adenovirus type 5 to stimulate efficient AAV protein expression.

From the triple-transfected cells, we then extracted total protein to monitor correct AAV protein expression, as well as extrachromosomal DNA to analyze vector DNA replication. A third aliquot of cells was lysed by repeated freeze-thawing to obtain crude extracts for AAV particle quantification.

The representative Western blots in Fig. 2a document that all helper plasmids properly expressed all AAV capsid proteins (also Rep; not shown) and illustrate our curious finding that all constructs expressed best in the presence of the AAV-5 genotype vector. Overall, the AAV-5 helper yielded the strongest expression, confirming our earlier observations (25). Interestingly, subsequent analysis of replicating vector DNA (Fig. 2b) showed that despite strong protein expression, the AAV-5 helper exclusively replicated the cognate AAV-5 vector plasmid but none of the five other genotypes. Vice versa, the five non-5 helper plasmids equally efficiently amplified all non-5 vector DNAs but not the AAV-5 genotyped construct. This confirmed and extended earlier reports showing that mutual interactions of AAV-5 ITRs and Rep proteins are mandatory for efficient AAV-5 particle production (7, 25).

Importantly, none of the combinations of vector genotype and helper serotype improved the replication of the respective *gfp* cassette, compared to the AAV-2 prototype. This proved that AAV ITRs are interchangeable during this initial step in the viral life cycle, provided that AAV replication proteins from a cognate serotype are expressed in *trans*.

This idea was further corroborated by quantifying the encapsidated vector DNAs (Fig. 2c), where, similar to the replication assays, we found that all combinations of geno- and serotypes yielded comparable vector particle titers. Again, notable exceptions were all pairings of AAV-5 helper or vector plasmids with noncognate partners, which had not resulted in detectable particle production (note that cross-packaging of the AAV-5 vector into serotype capsids other than AAV-5 was not analyzed due to the lack of respective helpers; see the next section). We also noted a tendency for the AAV-3- and -6-based helper plasmids to give slightly lower titers, while use of the AAV-4 helper typically yielded a marginal increase, concordant with our previous observations (25). However, since all

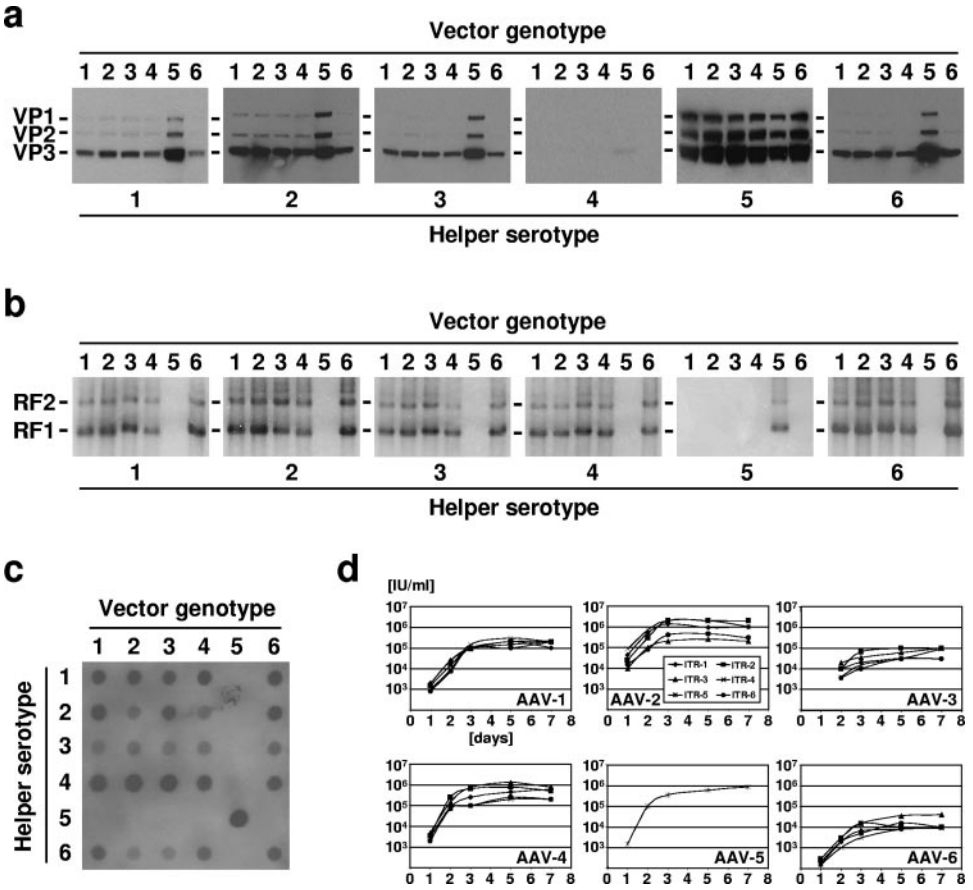

FIG. 2. In vitro characterization of AAV vector geno- and serotypes. (a) Western blot analysis. 293 cells were grown in 6-cm dishes and triple transfected with the following plasmids (2 μg each): an AAV vector plasmid carrying the *gfp* gene flanked by ITRs from genotypes 1 through 6, an AAV helper plasmid expressing *rep* and *cap* genes from AAV-1 to -6, and an adenoviral helper plasmid supplying functions required for AAV vector production. Three days later, the cells were harvested, washed once with 1× PBS, and aliquoted for analyses. Thus, a third of the total cells from a dish were lysed in protein extraction buffer, subjected to sodium dodecyl sulfate-polyacrylamide gel (12%) electrophoresis, and then Western blotted with the B1 antibody, which recognizes all three VP proteins (VP1, ~90 kDa; VP2, ~72 kDa; VP3, ~60 kDa) from AAV serotypes 1 to 3, 5 and 6 (25). The B1 epitope is only partially conserved in AAV-4, explaining the weak detection of respective capsid proteins. Note the generally strong expression of VP proteins from the AAV-5 helper and the drastically upregulated VP expression from all non-5 helpers when transfected together with the AAV-5 vector (for reasons unknown). (b) Southern blot analyses. A third of the cells from panel a were lysed by a modified Hirt procedure to release extrachromosomally replicated DNA, which was subsequently separated on 1% agarose gels and blotted with a radioactively labeled CMV probe. The two bands typically observed represented double-stranded monomer (RF1 [replication form 1], ~3.8 kb) and dimer (RF2, ~7.6 kb) vector DNA forms. (c) Dot blot titration. Shown is a representative blot demonstrating the large compatibility of non-5 helpers and vectors for particle production and, vice versa, the strict requirement for an AAV-5 helper to package the AAV-5 vector. (d) Transduction of cultured cells. HeLa cells were grown in 96-well plates and infected with 10-fold serial dilutions of the various AAV geno- and serotype preparations (the serotype is indicated in the lower right corner of each panel). Up to 1 week postinfection, Gfp-expressing cells were counted and titers of infectious units ([IU/ml]) calculated (shown are mean values from four titrations per vector; error bars have been omitted for clarity). The plots show that particle infectivity depended on and varied with the capsid serotype, not the vector genotype.

titer variations were within a fivefold range, we concluded that, as for genome amplification, AAV ITR origin is also irrelevant for vector DNA encapsidation.

We next asked whether the presence of specific genotype ITRs would alter the transduction profile of a given serotype in cultured cells. We therefore infected HeLa cells with identical total particle numbers of each geno- and serotyped *gfp* vector and counted Gfp-expressing cells at various time points after inoculation. The results, as shown in Fig. 2d, demonstrated no difference among the six ITRs, as long as they were delivered by the same viral shell. This proved that, in cultured cells, the major determinant of transduction efficacy with AAV is the viral serotype, not the vector genotype.

Cross-packaging of genotyped AAV-hFIX vector DNAs into AAV-8. We next addressed our main goal, which was to compare the six AAV genotypes for their performance in mouse liver. Therefore, we decided to pseudotype the six hFIX-encoding vector DNAs with AAV-8, based on recent work by us and others showing very high liver transduction efficiencies with this particular capsid (21, 38, 63).

An initial hurdle we had to overcome was the general lack of an AAV helper plasmid expressing AAV-8 VP together with AAV-5 Rep proteins, with the latter needed to replicate and package the AAV-5-genotyped vector DNA (7). We thus devised a PCR strategy to amplify and clone these two genes, resulting in a set of eight constructs in which AAV-5 *rep* and

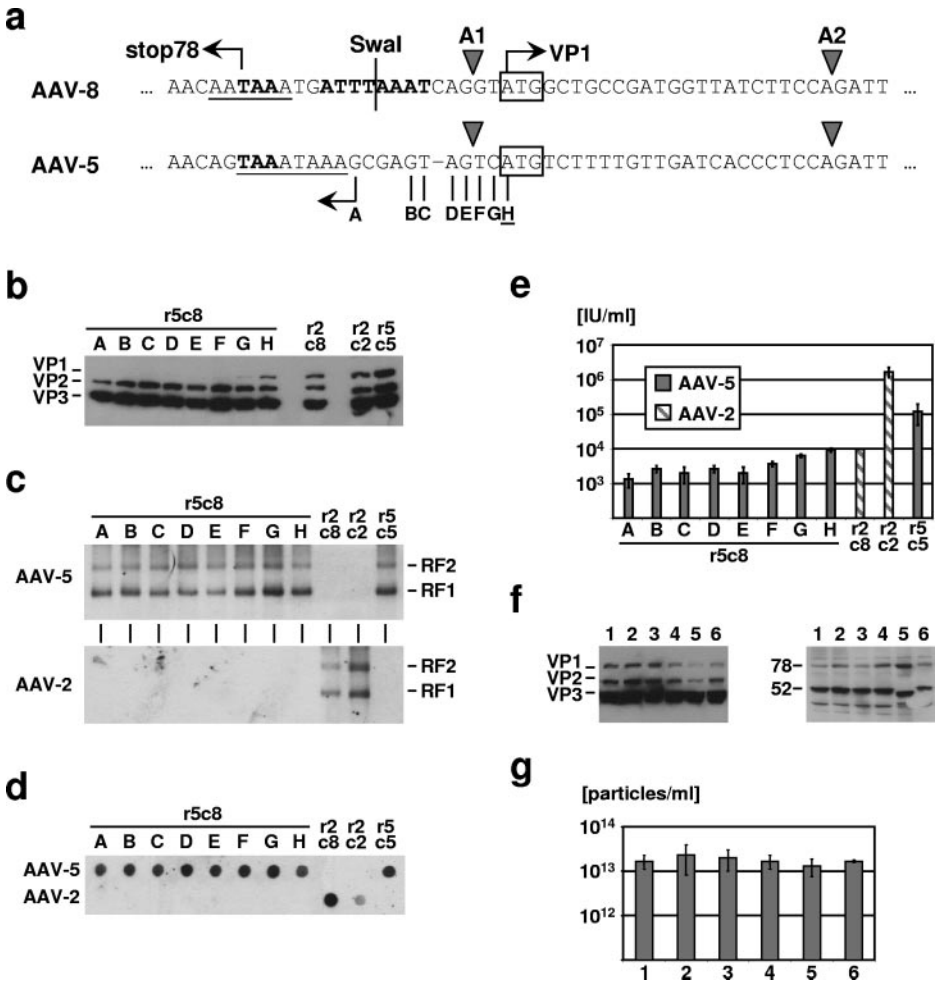

FIG. 3. Generation and characterization of a novel hybrid AAV-5/-8 packaging helper. (a) Sequence of the junction site of the AAV-5 *rep* and AAV-8 *cap* genes. Shown are the DNA sequences of an AAV-2/-8 helper plasmid (p5E18V2/8) or wild-type AAV-5 between the Rep78(/52) stop and VP1 start codons. The SwaI site highlighted in the AAV-2/-8 plasmid was used for fusion with the PCR-amplified AAV-5 *rep* gene. Arrows indicate the minor and major splice acceptor sites (A1 and A2) flanking the AAV-5 and -8 introns, while letters A through H depict the first nucleotides bound to the eight different PCR primers used to amplify AAV-5 *rep* (see Materials and Methods). Putative poly(A) signals within the AAV introns are underlined. (b) Western blot analyses. 293 cells were triple transfected with the AAV-2-based *gfp* vector plasmid, together with each of the eight hybrid AAV-5/-8 helpers from panel a and the adenoviral plasmid. Three days later, cells were lysed and AAV-8 VP proteins detected via Western blotting with the B1 antibody. Note that out of the eight hybrid constructs, only plasmid H properly expressed all three AAV-8 capsid proteins (VP1 to -3), as evident from comparison with control helpers expressing AAV-8, -2, or -5 VP protein (right lanes). (c) Southern blot analyses. Transfections were carried out as described for panel b, with a vector plasmid based on AAV-2 or -5, and replicated vector DNA was extracted and analyzed as for Fig. 2b. The blots show that all hybrid constructs equally efficiently replicated the AAV-5 vector while, as expected, the AAV-2-based control plasmid was only amplified by non-5 helpers expressing AAV-2 Rep proteins (r2). RF, replication forms. (d) Dot blot titration. Aliquots from the cells from panel c were lysed and AAV particle titers determined by dot blotting with a CMV-specific probe. In line with the DNA replication data from panel c, all eight hybrid helpers had efficiently packaged the AAV-5 vector but not the AAV-2 counterpart. Vice versa, the two AAV-2 Rep-expressing control helpers had only packaged the AAV-2 genotype but not AAV-5. (e) Quantification of infectious titers. The lysates from panel d were assayed for infectious AAV particles by diluting them on 293 cells and counting Gfp-expressing cells 3 days later. Among the eight hybrid helpers, clone H gave the highest infectious particle titers, which were identical to those obtained with a conventional AAV-2/-8 helper and an AAV-2 vector. Note that the infectious titers obtained with the r2c2 and r5c5 helpers (expressing Rep and VP from AAV-2 or -5) were the highest overall, due to the greater infectability of 293 cells with AAV serotypes 2 and 5, compared to serotype 8. Data are means ± standard deviations ($n = 3$). (f) Western blot analyses. The six *hfIX* vector genotypes (indicated by numbers above the blots) were packaged into AAV-8 with the novel hybrid AAV-5/-8 helper H (AAV-5 vector) or a conventional AAV-2/-8 helper (all other genotypes). Expression of AAV Rep (only Rep78 and Rep52 are marked) and VP proteins was monitored with 303.9 or B1 antibodies, respectively. (g) Dot blot titration of genotyped AAV-8 (*hfIX*). Shown are average particle titers ± standard deviations ($n = 3$) obtained from pseudotyping the six genotype vectors (numbers below the graph) with AAV-8 by using helpers as described for panel f.

AAV-8 *cap* were fused as shown in Fig. 3a. Our rationale for making multiple fusions stemmed from the fact that AAV-5 transcript splicing varies drastically from that of other AAV isolates (51–53), suggesting that maintaining part or all of the 3′ end of the AAV-5 *rep* open reading frame was key to preserving proper gene expression.

In fact, Western blot analysis of protein from transfected 293 cells revealed that only one (clone H) out of the eight different

PCR products expressed all three AAV-8 capsid proteins at the expected ratios (Fig. 3b). In all other cases, the largest protein (VP1) was either underrepresented (clones F and G) or completely absent (clones A to E). Interestingly, all eight plasmids equally efficiently supported replication of the AAV-5-based vector (Fig. 3c) and yielded similar amounts of total DNA-containing virions (Fig. 3d), indicating that VP1 expression is not required for these processes. On the other hand, VP1-expressing clone H resulted in the highest infectious particle titers of the eight plasmids, which were in fact indistinguishable from titers obtained with an AAV-2-based control vector and a standard AAV-2/-8 packaging helper (Fig. 3e).

Together, this showed that AAV-8 VP1 expression is irrelevant for AAV vector DNA replication and encapsidation but is crucial for the infectivity of assembled virions.

Consequently, to pseudotype the six *hfIX* genotypes with AAV-8 for subsequent in vivo analyses, we used the conventional AAV-2/-8 helper for encapsidation of genotypes 1 to 4 and 6 or our novel AAV-5/-8 helper H for the AAV-5 genotype. Particle production was monitored by Western blot analysis (Fig. 3f), verifying that both helpers expressed comparable amounts of AAV-8 VP proteins in the correct stoichiometry, as well as by dot blot quantification, showing consistently high packaging efficiencies with a less-than-fivefold variation in DNA-containing particle titers among all genotypes (Fig. 3g).

In vivo comparison of genotyped hFIX-expressing vector genomes from AAV-8. The six genotyped AAV-8 (*hfIX*) vector preparations were next administered to 6-week-old female C57BL/6 mice by using portal vein injections to maximize liver gene transfer. Each recombinant virus was injected at three different doses, low (5×10^{10} particles per mouse), medium (3×10^{11} particles per mouse), and high (1.8×10^{12} particles per mouse), with four to eight mice per group. Plasma was then collected over a period of 6 months, and hFIX levels were quantified via ELISA.

Three main findings were apparent from the data, as shown in Fig. 4. First, with all of the doses, hFIX expression from all six vectors gradually increased to a peak between 2 and 4 weeks postinjection but then declined thereafter to stabilize at significantly lower levels. These stable levels represented ~40% of the peak levels (low dose) or 17 or 10% (medium or high dose, respectively). Similar expression profiles, characterized by an early peak and a later dose-dependent decline, were found before (38, 58) and appear to be specific for AAV-8, as they are not seen with other AAV serotypes (see Discussion).

A second intriguing observation concerns the overall expression levels from the vectors; average peak levels in mice injected with the high vector doses reached 511 μg/ml hFIX, or 674 μg/ml in individual animals. To our knowledge, this is by far the strongest in vivo hFIX expression obtained with an AAV vector thus far, exceeding previously reported levels achieved with AAV serotypes by a factor of 3 (200 μg/ml with AAV-8) (38) or greater than 5 (135 μg/ml with AAV-6) (28). Notably, the peak levels found here would correspond to more than 10,000% of normal levels (5 μg/ml) in humans and would thus considerably exceed curative levels in hemophilic individuals.

The third result, and most intriguing in the context of the present work, was our finding of indistinguishable transduction profiles among the six genotypes when administered at identical doses. Thus, all constructs yielded the same initial rises in hFIX expression levels to reach the dose-specific peaks and then likewise showed identical declines and eventual stabilization. This corroborated our initial in vitro results (Fig. 2d) and thus led us to conclude that AAV ITR genotypes are restricting neither the transduction of cultured cells nor that of hepatocytes in vivo.

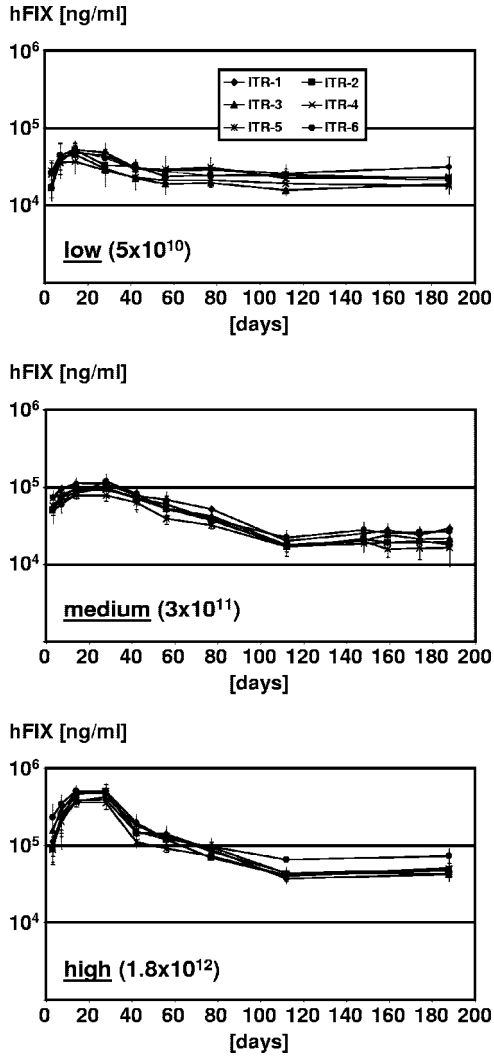

FIG. 4. In vivo hFIX expression from genotyped AAV-8 vectors. Mice were injected with the six genotyped hFIX expression vectors under the conditions and at the doses described in the text. Plasma was collected via retro-orbital bleeding, and hFIX levels were determined with a standard ELISA. Data are means ± standard deviations (n = 4 or 8).

Analysis of molecular forms of genotyped AAV vector DNA in stably transduced liver. Our finding of identical hFIX protein expression profiles within a dose cohort, regardless of the vector genotype, suggested that the six different constructs had persisted at equal genome copy numbers per cell. To verify this idea, we extracted total liver DNA from stably transduced mice 6 months after vector injection and assessed vector copy numbers via Southern blot analysis (Fig. 5a and b). Indeed, we found no statistically significant differences in vector copy

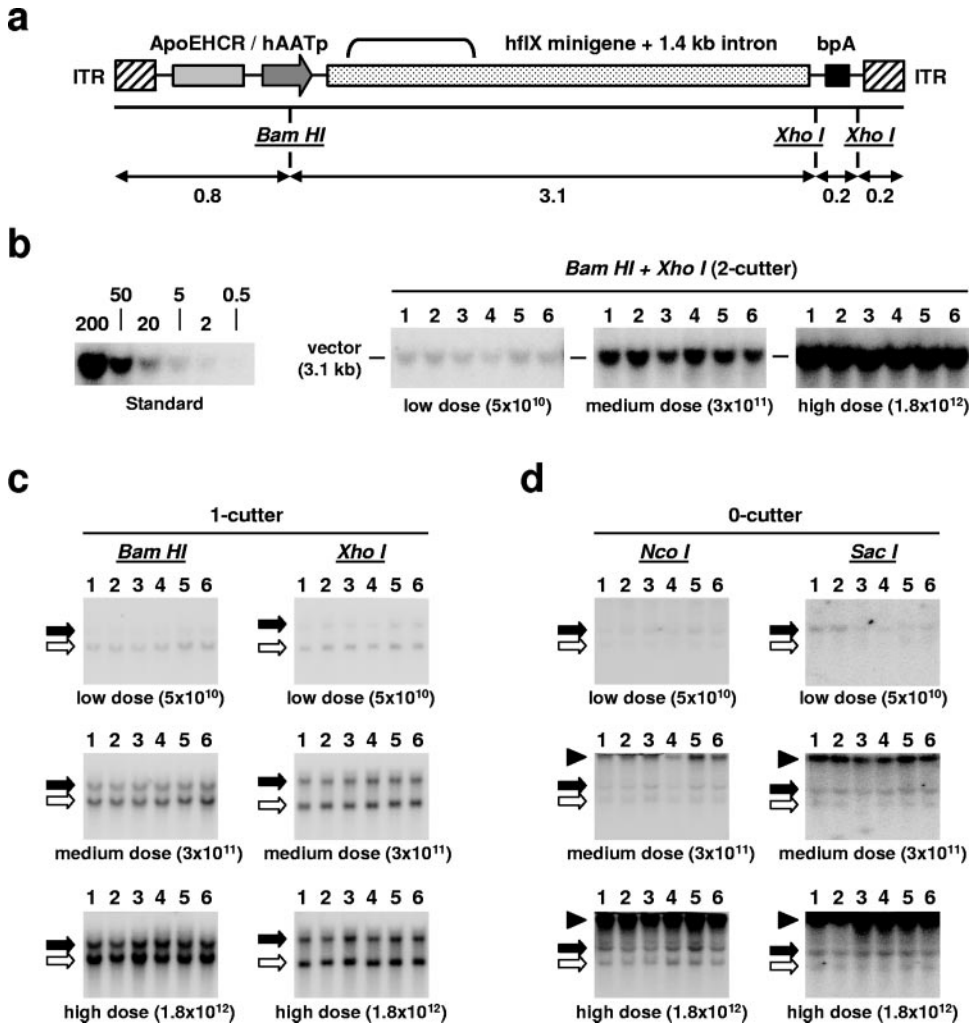

FIG. 5. Quantification and structural analyses of AAV genotypes in stably transduced hepatocytes. (a) Scheme of the AAV-2 *hfIX* vector DNA. Shown are the genetic structure of the recombinant *hfIX* expression cassette and the locations of the BamHI and XhoI restriction sites used for digestion in the panels below. The numbers below the arrows indicate fragment sizes in kilobases. ApoEHCR, apolipoprotein E enhancer with hepatic locus control region; bpA, bovine growth hormone poly(A) signal. (b) Quantification of vector genome copy numbers. Total liver DNA was extracted 6 months after vector administration, and 10 μg of DNA was analyzed by Southern blotting with BamHI/XhoI double digestion and a 4.04-kb *hfIX* probe. A double-stranded vector copy number standard curve was prepared by adding the corresponding amount of *hfIX* AAV-2 vector plasmid to 10 μg of liver DNA from a naive mouse. Each lane represents an individual mouse. (c) Analysis of molecular vector DNA forms. The DNAs from panel a were digested with restriction enzymes cutting the vector DNA once near the 5′ (BamHI) or 3′ (XhoI, two sites in close proximity) end and then separated and detected as described above. Open arrows indicate head-to-tail molecules, while solid arrows depict tail-to-tail (BamHI) or head-to-head (XhoI) forms. Alternatively (d), the same DNAs were digested with the shown noncutter enzymes and probed to visualize supercoiled or relaxed circular monomers (open or solid arrows, respectively) or high-molecular-weight concatemers (arrowheads).

numbers among the six genotypes within the dose groups, with average numbers of 8.1 ± 0.9, 46.6 ± 6.3, and 199 ± 32 double-stranded vector genomes per cell for the low, medium, and high doses, respectively. The finding of identical and genotype-independent vector copy numbers confirmed our hFIX protein expression data and thus further substantiated our novel model, according to which stable liver transduction with AAV vectors is not restricted by the vector genotype.

It remained an interesting possibility that the six genotype vectors had assumed unique molecular forms within the transduced hepatocytes, despite persisting at identical total copy numbers. Therefore, we resolved the structures of the different vector molecules by subjecting total liver DNA to complete digestion with various restriction enzymes, each cutting the AAV vector genome once. Subsequent Southern blot analyses of the products showed no differences in the manifestation of molecular forms among the genotypes; in fact, all six ITR variants had predominantly persisted as head-to-tail, or to a lesser extent also tail-to-tail, molecules (Fig. 5c).

The latter (tail-to-tail) molecules are typically indicative of concatemer formation, while head-to-tail molecules include both circular monomers and concatemers (45). To further distinguish these forms, we digested the liver DNAs with various noncutter enzymes. Subsequent Southern blot analyses (Fig. 5d) showed that, regardless of the genotype, all vectors had mostly persisted as episomal circular monomers at the low dose, while

TABLE 1. Liver transduction with AAV genotypes: hFIX expression levels and vector DNA copy numbers[c]

Vector dose	Total copy no./cell[d]	Relative amt of each vector form (%)[a]		hFIX level (μg/ml)[e]		Ratio of total vector copy no. to:		Ratio of monomer vector copy no.[b] to:	
		Circular monomer	Concatemer	Peak	Stable[f]	Peak hFIX	Stable hFIX	Peak hFIX	Stable hFIX
5×10^{10}	8.1 ± 0.9	93	7	58.2 ± 8.8	23.0 ± 3.3 (40)	0.14	0.35	0.13	0.33
3×10^{11}	46.6 ± 6.3	19	81	129.5 ± 13.3	22.5 ± 4.1 (17)	0.36	2.07	0.07	0.39
1.8×10^{12}	199 ± 32	10	90	511.1 ± 32.2	50.8 ± 6.8 (10)	0.39	3.92	0.04	0.39

[a] Relative amounts of circular monomers and concatemers in each sample were estimated by densitometry of the Southern blots shown in Fig. 5d. For more details and limitations of this estimation, see reference 41.
[b] Monomer copy numbers per cell were deduced by multiplying the total vector copy number per cell (second column) by the relative amount of circular monomers (third column)/100. For limitations of this calculation, see reference 41.
[c] Shown throughout the table are average data ± the standard deviation per vector dose for all six genotypes (there were no significant differences in copy numbers, molecular forms, or hFIX expression among the six vectors; see text for details).
[d] Vector copy numbers per cell (i.e., per diploid genomic equivalent) were calculated by densitometry of the Southern blots shown in Fig. 5b.
[e] Peak and stable hFIX levels were obtained between weeks 2 and 4, or month 6, postinfection, respectively (see also Fig. 4).
[f] Values in parentheses indicate percentages of stable hFIX levels of initial peak levels.

at higher doses they had formed concatemers. Importantly, this shift to higher-molecular-weight forms occurred independently of ITR origin.

A summary of our findings on AAV DNA vector copy numbers and molecular forms, together with the respective hFIX expression data, is presented in Table 1.

AAV DNA persists predominantly episomally regardless of the vector genotype. Our final interest was to determine whether the concatemers observed at the medium or high dose represented mostly episomal or integrated sequences and whether the distribution was genotype specific. Therefore, we performed partial two-thirds hepatectomies on individual mice from the six medium-dose groups 5 months after the injection, when hFIX levels had already reached a stable plateau (Fig. 4). As first reported by Nakai et al., this surgical procedure typically results in an ~90% drop in protein expression levels from AAV-2-based vectors, along with a similar reduction in vector copy numbers (45). This is due to the predominantly episomal persistence of AAV-2 vectors and their subsequent loss during the process of liver regeneration and hepatocyte division.

Here we found such drops in protein levels and copy numbers to occur in all six groups, regardless of the vector genotype. Figure 6a shows that hFIX protein levels consistently fell to ~20% of the pretreatment level within days after surgery and remained low for more than 1 month. This strongly suggested that all six genotypes had mainly persisted as episomes and thus been diluted out during cell cycling due to the liver regenerative process.

This was directly confirmed by Southern blot analyses with total genomic DNA extracted from livers removed at the time of surgery or recovered from the same mice 6 weeks later, at a time when the organs had fully regenerated (45). As evident from Fig. 6b, there was a dramatic reduction in AAV vector copy numbers for all genotypes, substantiating our finding that all six vectors had predominantly persisted as nonintegrated molecules, likely circular monomers or larger concatemers (Fig. 5d).

DISCUSSION

This study was designed to address an aspect of the widely used AAV pseudotypes that we felt has largely been overlooked in the past, i.e., the role of the genotype of the ITRs flanking the recombinant DNA. In fact, nearly all of the AAV vector DNAs pseudotyped to date were based on the AAV-2 prototype, which seems paradoxical considering that ITRs from at least eight different AAVs were cloned or sequenced thus far (4, 8, 9, 55, 59, 68). Perhaps this was mostly due to practical reasons, in particular, the limited availability of genotyped vector plasmids which are as flexible and convenient as the many existing AAV-2 variants. To our knowledge, only

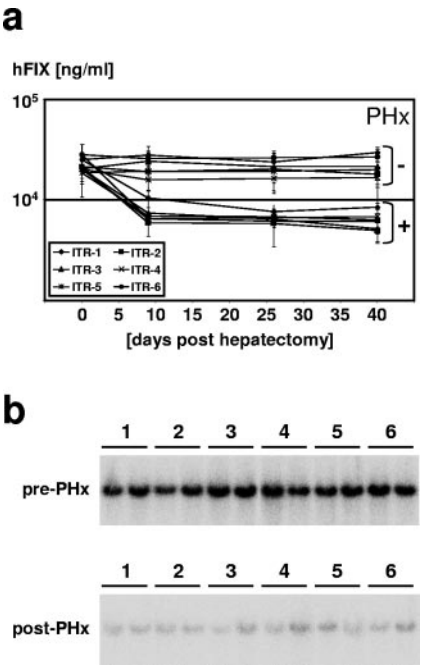

FIG. 6. Evidence for episomal persistence of AAV vector genotypes. Mice ($n = 3$) from the six medium-dose groups were subjected to partial hepatectomies 5 months after vector administration to induce liver regeneration and loss of nonintegrated AAV vector DNA. (a) hFIX measurements. Plasma hFIX levels were determined at the time of hepatectomy (PHx) and then up to 6 weeks after. Data are means ± standard deviations. (b) Quantification of AAV vector copy numbers in hepatectomized mice. Vector DNA copy numbers were determined in livers taken at the time of hepatectomy or 6 weeks later. Shown are two representative mice per group, with numbers above the blots indicating vector genotypes. For details and a standard curve, see Fig. 5b.

four other genotypes were ever vectorized at all (AAV-3, -5, and -6 and AAAV), and in each case there is only one reported clone (4, 8, 55). Hence, for analyses of the complete set of ITRs from AAV-1 through -6, we had to de novo synthesize AAV-1 and -4 ITRs based on published sequences. The two resulting plasmids should be useful tools for future studies of genotyped AAV vector DNAs.

A second hurdle was specifically posed by AAV-5, which due to its unique ITR composition requires expression of AAV-5 Rep proteins from the packaging helper (7). However, the only such helper reported in the literature also expresses AAV-5 capsid proteins, explaining why the AAV-5 genotype was exclusively studied from cognate viral shells so far and creating a need for novel plasmids permitting its pseudotyping for a broader evaluation.

To fill in this gap was our first goal, based on our previous finding of poor performance of the AAV-5 capsid in our tissue of interest, murine liver (28). We therefore developed a new hybrid helper expressing AAV-8 capsid proteins together with AAV-5 Rep to pseudotype AAV-5 and the other five genotypes with a superior shell. Interestingly, we found that only one of our eight constructs (clone H) expressed all capsid proteins at the correct stoichiometry. This was, however, not surprising in view of earlier reports showing that AAV-5 is not only unique in its ITR, but also the intron, particularly the minor splice acceptor site (A1 in Fig. 3a) (51–53). We thus assume that inexact fusion of the AAV-5 *rep* and AAV-8 *cap* genes in the seven other constructs prevented proper use of the A1 site, disrupting correct splicing and consequently VP1 expression. A second interesting finding was that while all constructs replicated and packaged the AAV-5 vector, clone H yielded the most infectious particles. Since the eight plasmids mainly differed in VP1 expression, we speculate that, similar to AAV-2 (2, 22, 31), the phospholipase 2A domain in the VP1 N terminus is crucial for AAV-8 particle infectivity. This is a novel finding which underscores the central role of this particular domain for the AAV life cycle.

The successful generation of an AAV-5/-8 pseudotyping helper allowed a fair comparison of the six AAV genotypes in vivo. We had two expectations based on our initial in vitro data and our previous work. First, the small-scale packaging of the *gfp* genotypes suggested that, with the appropriate AAV-2/-8 or -5/-8 hybrid helpers, all *hfIX* ITR variants would amplify and encapsidate equally efficiently. This was in fact what we observed and what led us to conclude that ITRs are freely interchangeable for AAV DNA replication and encapsidation, as long as cognate Rep proteins are expressed from the helper. Our findings moreover argue against a role for an exact *rbs* sequence or length, as previously postulated for AAV-4 (9), because replication or packaging advantages were not evident for any particular genotype. Notably, we observed slightly improved packaging of all vector genotypes when coexpressing the AAV-4 Rep and capsid proteins, corroborating our previous observations (25) and suggesting a particularly strong AAV-4 protein interaction during DNA uptake.

A second hypothesis was that the vector genotype would not affect early in vivo transgene expression from the six *hfIX* viruses. This was implied by the nearly identical short-term profiles observed in cultured cells infected with the *gfp* genotypes, which had suggested a hierarchy of the viral serotype over the vector genotype in early transduction. It still seemed possible that results would differ in vivo, where we targeted a distinct cell type (hepatocytes), used another serotype (AAV-8), and most importantly followed transgene expression for a much longer period (6 months). Nonetheless, our key observation in this study was that the kinetics, levels, and persistence of in vivo hFIX expression were identical among all groups. Likewise, we found that all six ITR variants persisted at equal copy numbers and molecular forms and mostly episomally.

Our central conclusion from these findings is that in vivo liver transduction with AAV is not restricted by the vector genotype but only by the viral serotype. To further support this idea, we can compare the current hFIX levels to those of a previous report from our group (28). Pseudotyping the same AAV-2-based *hfIX* vector DNA with AAV-2 (previously) or AAV-8 (here) resulted in fivefold higher hFIX peak levels under identical experimental conditions (mouse strain, vector dose, delivery route). Moreover, we noted a dramatic change in the transduction profiles between the two studies. Thus, in contrast to the stable hFIX profiles from serotypes 1 through 6 in our previous report (28), we now observed an early hFIX peak with the AAV-8 capsid, followed by a dose-dependent decline to lower steady-state levels. The fact that these profiles were independent of the genotype clearly indicated a correlation with the viral shell and not the ITRs.

Importantly, these findings can easily be reconciled with our previously established model for liver transduction with AAV-2. Accordingly, a hallmark is that the hepatocytes were all capable of virus uptake since vector DNA was typically found in nearly 100% of the cells already at a low dose of 10^{11} AAV-2 particles. However, for reasons still unknown, transgene expression was confined to only 10% of the hepatocytes, regardless of the AAV-2 particle dose (33, 43, 62). In contrast, the AAV-8 shell or, alternatively, delivery of self-complementary vector DNA alleviates the block in transduction and yields expression in the entire liver (38, 63; unpublished data). Our model proposes that gene transfer with inefficient capsids (e.g., AAV-2) is primarily impaired at the level of post-particle entry by an obstacle upstream of gene expression. A comparison of serotypes 2 and 8 showed that the rate-limiting step is uncoating of the vector DNA, which restricts the intracellular levels of plus and minus single-stranded input DNAs (63) and subsequently their conversion to stable, transcriptionally active duplex forms, which we believe occurs via annealing of complementary single strands (42, 63).

This model predicts that genetic factors such as ITR sequences are irrelevant for the early steps of liver transduction, since all input DNAs share the common block in duplex annealing. Yet this is only applicable when they are present in identical concentrations and when capsid-related artifacts such as particle uptake, trafficking, or nuclear entry are eliminated. Importantly, this was guaranteed here by using the AAV-8 capsid to transfer all six genotypes, and this also distinguishes our work from previous studies, where various capsids were used to deliver genotypes, hence mimicking potential effects from the ITRs (e.g., reference 10).

Our observation of identical expression levels from all six genotypes from the same capsid is fully consistent with the DNA annealing model. Accordingly, we speculate that all vector DNAs were rapidly uncoated from the AAV-8 shells and

thus present in high concentrations, resulting in fast annealing to biologically active duplex DNAs and the observed early onset of hFIX expression. We believe that the ITRs were not significantly determining this process, as we did not see any difference among the six groups.

Notably, strand annealing is just one possible mechanism for duplex conversion. Others proposed a second-strand DNA synthesis model where the ITRs serve as primers for DNA polymerase (15, 16, 57). Our data are also concordant with this alternative model, since despite DNA sequence divergence, all six ITRs can assume a secondary hairpin structure. We thus still believe the ITR sequence to be irrelevant, as secondary structure suffices to comply with the replication model. Interestingly, a hallmark of this model is ITR binding by regulatory proteins which prevent processing of DNA polymerase (47–50). Initially discovered for AAV-2, one would have to assume similar binding of these proteins to alternative ITRs to postulate a general role in regulating AAV strand conversion. Considering that the known ITRs differ significantly outside the *rbs* and *trs*, and thus in the presumed protein binding sites, we therefore favor the more general and ITR-independent mechanism of single-strand annealing over second-strand synthesis.

To further distinguish between the two models, it would help to study synthetic and unique ITRs, conserving only *rbs* and *trs* sequences, as well as the hairpin nature. Our present findings suggest that encapsidating such synthetic ITRs will not be problematic, as we showed that the *rbs* and *trs* are the sole essential sequences for vector production.

Annealing (or replication) of single-stranded input DNA is just the early step in hepatocyte transduction and is typically followed by further conversion of the linear duplex molecule into a variety of episomal forms, mediating persistent transgene expression. These include linear and circular monomers and multimers, with circular monomers giving gene expression and larger concatemers being mostly biologically inactive (42, 43, 45). The two parameters determining the intracellular proportion of these forms are the virus dose and rate of uncoating, since both affect the levels of input single-stranded DNA or annealed linear duplex monomers (38, 42, 63). However, the role of the ITRs in in vivo genome conversion remains unclear and rather controversial.

Interestingly, we had previously compared naked duplex linear and circular DNA molecules, with or without ITRs, in murine liver and found that, regardless of ITRs, linear but not circular DNA is a main substrate for concatemerization (6, 37, 40, 54). The concatemers stemmed from random intermolecular recombination of linear duplex DNAs likely mediated by cellular DNA repair systems recognizing the free molecule ends as DNA damage signals (13, 41, 73). We also showed that the preferred pathway for removal of free AAV DNA ends is self-circularization, while concatemerization only occurs once this pathway's capacity is exceeded (41). This likely explains why AAV-8-transduced cells mostly accumulate large concatemers, in particular at higher doses, as seen before (38) and here. It could also explain the drop-off in expression with AAV-8 following an early peak, as the concatemers appear to be transcriptionally inactive (38).

This particular idea is indeed strongly supported by the sum of our data shown in Fig. 4 and 5 and Table 1. Thus, we found a correlation of total vector copy numbers and peak hFIX expression levels but a discrepancy between the former and stable hFIX levels (Table 1). In fact, total vector copy numbers increased more rapidly than stable hFIX levels at higher doses, suggesting that the majority of vector genomes were biologically inactive under those conditions. Interestingly, up to 90% of the total vector molecules were concatemers at the highest dose, implying that those large forms did not significantly contribute to gene expression. In contrast, we found a consistent correlation between circular molecule numbers and stable hFIX levels at all doses (Table 1, last column), supporting our belief that those smaller, episomal forms were actually mainly yielding hFIX expression in vivo. It is worth noting that an alternative explanation for the eventual drop-off in hFIX expression could come from induction of humoral or cellular immune responses in the transduced animals (46). This is unlikely, however, since we previously obtained stable expression of more than 100 μg/ml hFIX from other serotypes in the same mouse strain (28) and Sarkar et al. (58) reported similarly transiently elevated expression with an independent factor VIII-encoding AAV-8.

Based on our historic results with naked linear DNA (6, 37, 40, 41), we expected that the genotype would not affect AAV vector DNA persistence, and this is indeed what we observed. Analyses of molecular vector DNA forms confirmed that, dose dependently, all six vectors persisted as either duplex circular monomers (low doses) or high-molecular-weight concatemers (high doses). We are thus convinced that the different ITRs were merely recognized as linear free DNA ends and as such represented efficient substrates for self-circularization or, once this pathway was saturated at higher doses (41), for concatemerization.

Again, this model of AAV vector genome conversion via nonhomologous end joining is not exclusive and we cannot rule out a role for homologous recombination between specific ITR sequences. In fact, support for this alternative model comes from a recent study by Yan et al. (70), who found that hybrid vectors carrying ITRs from AAV-2 and -5 less efficiently formed monomer circular intermediates while showing higher rates of directional intermolecular recombination. Their studies were, however, restricted to cultured cells, leaving the molecular fate of such hybrid vectors in vivo to be determined. For this purpose, the novel ITR clones presented here, together with our strategy to pseudotype the AAV-5 genotype, should prove very useful.

Despite our conclusion that the AAV genotype is irrelevant in the liver, we believe that further investigation of various ITRs is crucial for the field. First, our results might be liver specific, and the outcome of switching genotypes could differ in other tissues, in particular in muscle, where circular and not linear duplex DNAs represent precursors for concatemerization (11–13, 71, 72). For circle formation, single-stranded input genomes anneal via the ITRs into a panhandle-like structure, followed by ITR recombination and second-strand synthesis (72), implying that the ITR sequence is more crucial in muscle. Second, we envision multiple benefits from alternative ITRs for AAV vector production. For instance, recent work showed that the AAAV ITR is inherently more stable than other genotypes and that AAAV Rep overexpression had no adverse effect on cells, together implying usefulness for vector development (4). Third, it will be interesting to study the impact of

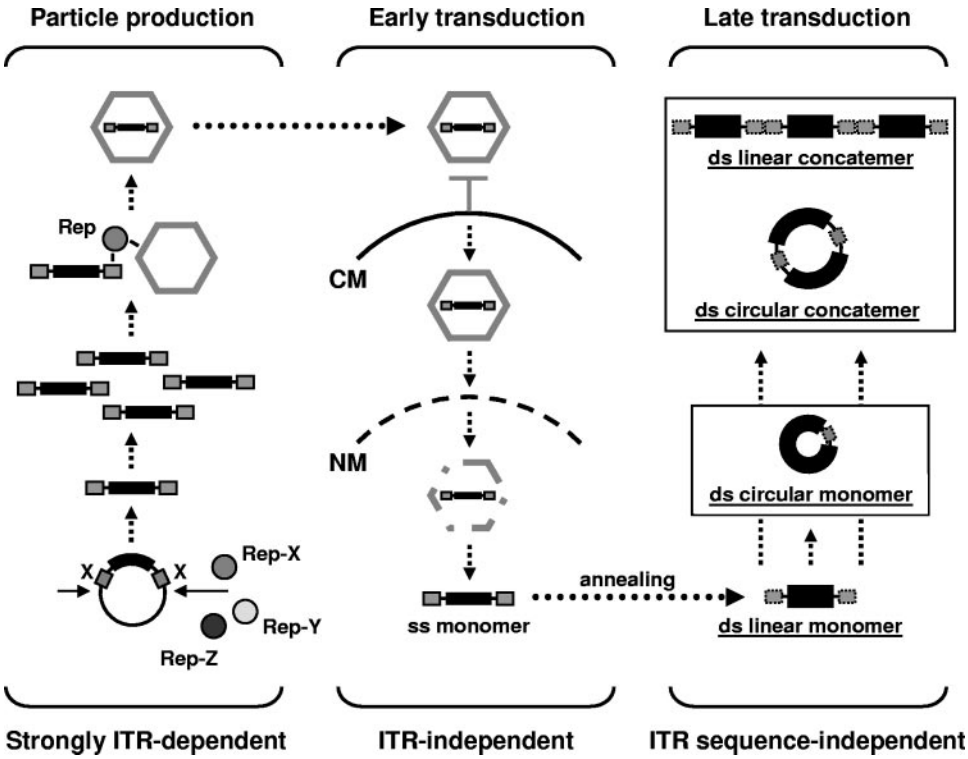

FIG. 7. Role of ITRs in the recombinant AAV life cycle. Shown are the various steps from production of recombinant viruses, including Rep-dependent vector DNA rescue, replication, and encapsidation (bottom to top), to early transduction, comprising particle uptake, trafficking, nuclear entry, and uncoating (top to bottom), to late transduction, with the multiple results from conversion of the single-stranded input DNA into higher-molecular-weight forms. Depicted are the linear and circular mono- and multimeric forms typically observed in the liver, with episomal concatemers predominating in AAV-8-transduced hepatocytes, although circular duplex monomers are mainly responsible for transgene expression (38, 63). As detailed in the Discussion, we hypothesize that for generation of any of these forms, AAV ITRs are largely redundant and that their genotype can be freely substituted, as visualized by drawing the ITRs with dotted lines. Not depicted are integrated vector DNA forms, due to the fact that they represent only a minority of all the molecules in AAV-transduced hepatocytes. CM, cellular membrane; NM, nuclear membrane; X, ITRs from genotype X; Rep-X/Y/Z, Rep proteins from various serotypes; ss, single-stranded; ds, double-stranded.

genotypes on vector DNA integration into the host genome. AAV-2 vectors integrate infrequently (<10%) and via existing duplex DNA breaks (34, 35, 39, 44) and thus in a random and ITR-independent fashion, although integration sites had microhomologies to the AAV-2 ITR and Nakai et al. identified a recombination hot spot in one ITR arm (44). It will be exciting to extend such studies to other AAV genotypes, in particular AAV-5, which as the wild type rarely integrates, if at all (U. Bantel-Schaal, personal communication). Translating this into vectors based on AAV-5 is a desirable goal, as it would relieve concerns of random DNA integration into the host genome. Finally, it will be interesting to study genotypes from capsids with lesser efficiencies of uncoating than AAV-8. In fact, we cannot rule out the possibility that the high efficacy of AAV-8 masked some ITR-specific effects in our study, such as intrinsic promoter activities, or binding of regulatory cellular proteins blocking second-strand synthesis or annealing. An important question for future work is whether these barriers can be overcome by switching to another genotype. An interesting additional candidate to include will be the AAV-8 ITRs, whose sequence was unknown at the time of our study but, it is hoped, will be available soon.

In summary, we have provided the first comprehensive side-by-side analyses of multiple AAV ITR genotypes, addressing all important steps of the AAV life cycle from in vitro vector production to in vivo liver transduction. We found a hierarchy of serotype over genotype and conclude that AAV ITRs are essential for vector production but later become dispensable and are irrelevant for persistent liver gene expression (Fig. 7). These results, together with the vector and helper plasmids reported here, support and facilitate the further evaluation of AAV ITRs in other models of in vivo gene transfer.

ACKNOWLEDGMENTS

We are grateful to James Wilson for providing AAV-2/-8 helper plasmid p5E18V2/8, as well as to Rob Kotin, Jay Chiorini, and David Russell for initial gifts of plasmids expressing AAV serotype 3 to 6 proteins or carrying ITRs from AAV-3, -5, or -6, respectively. We gratefully acknowledge help with mouse plasma collection by Efren P. Riu.

This work was supported by NIH grant HL66948 (M.A.K.).

REFERENCES

1. **Berns, K. I., and C. Giraud.** 1996. Biology of adeno-associated virus. Curr. Top. Microbiol. Immunol. **218:**1–23.
2. **Bleker, S., F. Sonntag, and J. A. Kleinschmidt.** 2005. Mutational analysis of narrow pores at the fivefold symmetry axes of adeno-associated virus type 2 capsids reveals a dual role in genome packaging and activation of phospholipase A2 activity. J. Virol. **79:**2528–2540.
3. **Bohenzky, R. A., R. B. LeFebvre, and K. I. Berns.** 1988. Sequence and symmetry requirements within the internal palindromic sequences of the adeno-associated virus terminal repeat. Virology **166:**316–327.

4. **Bossis, I., and J. A. Chiorini.** 2003. Cloning of an avian adeno-associated virus (AAAV) and generation of recombinant AAAV particles. J. Virol. **77:**6799–6810.
5. **Cathomen, T., T. H. Stracker, L. B. Gilbert, and M. D. Weitzman.** 2001. A genetic screen identifies a cellular regulator of adeno-associated virus. Proc. Natl. Acad. Sci. USA **98:**14991–14996.
6. **Chen, Z. Y., S. R. Yant, C. Y. He, L. Meuse, S. Shen, and M. A. Kay.** 2001. Linear DNAs concatemerize in vivo and result in sustained transgene expression in mouse liver. Mol. Ther. **3:**403–410.
7. **Chiorini, J. A., S. Afione, and R. M. Kotin.** 1999. Adeno-associated virus (AAV) type 5 Rep protein cleaves a unique terminal resolution site compared with other AAV serotypes. J. Virol. **73:**4293–4298.
8. **Chiorini, J. A., F. Kim, L. Yang, and R. M. Kotin.** 1999. Cloning and characterization of adeno-associated virus type 5. J. Virol. **73:**1309–1319.
9. **Chiorini, J. A., L. Yang, Y. Liu, B. Safer, and R. M. Kotin.** 1997. Cloning of adeno-associated virus type 4 (AAV4) and generation of recombinant AAV4 particles. J. Virol. **71:**6823–6833.
10. **Davidson, B. L., C. S. Stein, J. A. Heth, I. Martins, R. M. Kotin, T. A. Derksen, J. Zabner, A. Ghodsi, and J. A. Chiorini.** 2000. Recombinant adeno-associated virus type 2, 4, and 5 vectors: transduction of variant cell types and regions in the mammalian central nervous system. Proc. Natl. Acad. Sci. USA **97:**3428–3432.
11. **Duan, D., P. Sharma, J. Yang, Y. Yue, L. Dudus, Y. Zhang, K. J. Fisher, and J. F. Engelhardt.** 1998. Circular intermediates of recombinant adeno-associated virus have defined structural characteristics responsible for long-term episomal persistence in muscle tissue. J. Virol. **72:**8568–8577.
12. **Duan, D., Z. Yan, Y. Yue, and J. F. Engelhardt.** 1999. Structural analysis of adeno-associated virus transduction circular intermediates. Virology **261:**8–14.
13. **Duan, D., Y. Yue, and J. F. Engelhardt.** 2003. Consequences of DNA-dependent protein kinase catalytic subunit deficiency on recombinant adeno-associated virus genome circularization and heterodimerization in muscle tissue. J. Virol. **77:**4751–4759.
14. **Duan, D., Y. Yue, Z. Yan, and J. F. Engelhardt.** 2000. A new dual-vector approach to enhance recombinant adeno-associated virus-mediated gene expression through intermolecular cis activation. Nat. Med. **6:**595–598.
15. **Ferrari, F. K., T. Samulski, T. Shenk, and R. J. Samulski.** 1996. Second-strand synthesis is a rate-limiting step for efficient transduction by recombinant adeno-associated virus vectors. J. Virol. **70:**3227–3234.
16. **Fisher, K. J., G. P. Gao, M. D. Weitzman, R. DeMatteo, J. F. Burda, and J. M. Wilson.** 1996. Transduction with recombinant adeno-associated virus for gene therapy is limited by leading-strand synthesis. J. Virol. **70:**520–532.
17. **Flotte, T. R., S. A. Afione, R. Solow, M. L. Drumm, D. Markakis, W. B. Guggino, P. L. Zeitlin, and B. J. Carter.** 1993. Expression of the cystic fibrosis transmembrane conductance regulator from a novel adeno-associated virus promoter. J. Biol. Chem. **268:**3781–3790.
18. **Flotte, T. R., E. M. Schwiebert, P. L. Zeitlin, B. J. Carter, and W. B. Guggino.** 2005. Correlation between DNA transfer and cystic fibrosis airway epithelial cell correction after recombinant adeno-associated virus serotype 2 gene therapy. Hum. Gene Ther. **16:**921–928.
19. **Gao, G., M. R. Alvira, S. Somanathan, Y. Lu, L. H. Vandenberghe, J. J. Rux, R. Calcedo, J. Sanmiguel, Z. Abbas, and J. M. Wilson.** 2003. Adeno-associated viruses undergo substantial evolution in primates during natural infections. Proc. Natl. Acad. Sci. USA **100:**6081–6086.
20. **Gao, G., L. H. Vandenberghe, M. R. Alvira, Y. Lu, R. Calcedo, X. Zhou, and J. M. Wilson.** 2004. Clades of Adeno-associated viruses are widely disseminated in human tissues. J. Virol. **78:**6381–6388.
21. **Gao, G. P., M. R. Alvira, L. Wang, R. Calcedo, J. Johnston, and J. M. Wilson.** 2002. Novel adeno-associated viruses from rhesus monkeys as vectors for human gene therapy. Proc. Natl. Acad. Sci. USA **99:**11854–11859.
22. **Girod, A., C. E. Wobus, Z. Zadori, M. Ried, K. Leike, P. Tijssen, J. A. Kleinschmidt, and M. Hallek.** 2002. The VP1 capsid protein of adeno-associated virus type 2 is carrying a phospholipase A2 domain required for virus infectivity. J. Gen. Virol. **83:**973–978.
23. **Grimm, D.** 2002. Production methods for gene transfer vectors based on adeno-associated virus serotypes. Methods **28:**146–157.
24. **Grimm, D., and M. A. Kay.** 2003. From virus evolution to vector revolution: use of naturally occurring serotypes of adeno-associated virus (AAV) as novel vectors for human gene therapy. Curr. Gene Ther. **3:**281–304.
25. **Grimm, D., M. A. Kay, and J. A. Kleinschmidt.** 2003. Helper virus-free, optically controllable, and two-plasmid-based production of adeno-associated virus vectors of serotypes 1 to 6. Mol. Ther. **7:**839–850.
26. **Grimm, D., A. Kern, M. Pawlita, F. Ferrari, R. Samulski, and J. Kleinschmidt.** 1999. Titration of AAV-2 particles via a novel capsid ELISA: packaging of genomes can limit production of recombinant AAV-2. Gene Ther. **6:**1322–1330.
27. **Grimm, D., K. Pandey, and M. A. Kay.** 2005. Adeno-associated virus vectors for short hairpin RNA expression. Methods Enzymol. **392:**381–405.
28. **Grimm, D., S. Zhou, H. Nakai, C. E. Thomas, T. A. Storm, S. Fuess, T. Matsushita, J. Allen, R. Surosky, M. Lochrie, L. Meuse, A. McClelland, P. Colosi, and M. A. Kay.** 2003. Preclinical in vivo evaluation of pseudotyped adeno-associated virus vectors for liver gene therapy. Blood **102:**2412–2419.
29. **Halbert, C. L., E. A. Rutledge, J. M. Allen, D. W. Russell, and A. D. Miller.** 2000. Repeat transduction in the mouse lung by using adeno-associated virus vectors with different serotypes. J. Virol. **74:**1524–1532.
30. **Im, D. S., and N. Muzyczka.** 1989. Factors that bind to adeno-associated virus terminal repeats. J. Virol. **63:**3095–3104.
31. **Kronenberg, S., B. Bottcher, C. W. von der Lieth, S. Bleker, and J. A. Kleinschmidt.** 2005. A conformational change in the adeno-associated virus type 2 capsid leads to the exposure of hidden VP1 N termini. J. Virol. **79:**5296–5303.
32. **Liu, M., Y. Yue, S. Q. Harper, R. W. Grange, J. S. Chamberlain, and D. Duan.** 2005. Adeno-associated virus-mediated microdystrophin expression protects young mdx muscle from contraction-induced injury. Mol. Ther. **11:**245–256.
33. **Miao, C. H., H. Nakai, A. R. Thompson, T. A. Storm, W. Chiu, R. O. Snyder, and M. A. Kay.** 2000. Nonrandom transduction of recombinant adeno-associated virus vectors in mouse hepatocytes in vivo: cell cycling does not influence hepatocyte transduction. J. Virol. **74:**3793–3803.
34. **Miller, D. G., L. M. Petek, and D. W. Russell.** 2004. Adeno-associated virus vectors integrate at chromosome breakage sites. Nat. Genet. **36:**767–773.
35. **Miller, D. G., E. A. Rutledge, and D. W. Russell.** 2002. Chromosomal effects of adeno-associated virus vector integration. Nat. Genet. **30:**147–148.
36. **Mori, S., L. Wang, T. Takeuchi, and T. Kanda.** 2004. Two novel adeno-associated viruses from cynomolgus monkey: pseudotyping characterization of capsid protein. Virology **330:**375–383.
37. **Nakai, H., S. Fuess, T. A. Storm, L. A. Meuse, and M. A. Kay.** 2003. Free DNA ends are essential for concatemerization of synthetic double-stranded adeno-associated virus vector genomes transfected into mouse hepatocytes in vivo. Mol. Ther. **7:**112–121.
38. **Nakai, H., S. Fuess, T. A. Storm, S. Muramatsu, Y. Nara, and M. A. Kay.** 2005. Unrestricted hepatocyte transduction with adeno-associated virus serotype 8 vectors in mice. J. Virol. **79:**214–224.
39. **Nakai, H., E. Montini, S. Fuess, T. A. Storm, M. Grompe, and M. A. Kay.** 2003. AAV serotype 2 vectors preferentially integrate into active genes in mice. Nat. Genet. **34:**297–302.
40. **Nakai, H., E. Montini, S. Fuess, T. A. Storm, L. Meuse, M. Finegold, M. Grompe, and M. A. Kay.** 2003. Helper-independent and AAV-ITR-independent chromosomal integration of double-stranded linear DNA vectors in mice. Mol. Ther. **7:**101–111.
41. **Nakai, H., T. A. Storm, S. Fuess, and M. A. Kay.** 2003. Pathways of removal of free DNA vector ends in normal and DNA-PKcs-deficient SCID mouse hepatocytes transduced with rAAV vectors. Hum. Gene Ther. **14:**871–881.
42. **Nakai, H., T. A. Storm, and M. A. Kay.** 2000. Recruitment of single-stranded recombinant adeno-associated virus vector genomes and intermolecular recombination are responsible for stable transduction of liver in vivo. J. Virol. **74:**9451–9463.
43. **Nakai, H., C. E. Thomas, T. A. Storm, S. Fuess, S. Powell, J. F. Wright, and M. A. Kay.** 2002. A limited number of transducible hepatocytes restricts a wide-range linear vector dose response in recombinant adeno-associated virus-mediated liver transduction. J. Virol. **76:**11343–11349.
44. **Nakai, H., X. Wu, S. Fuess, T. A. Storm, D. Munroe, E. Montini, S. M. Burgess, M. Grompe, and M. A. Kay.** 2005. Large-scale molecular characterization of adeno-associated virus vector integration in mouse liver. J. Virol. **79:**3606–3614.
45. **Nakai, H., S. R. Yant, T. A. Storm, S. Fuess, L. Meuse, and M. A. Kay.** 2001. Extrachromosomal recombinant adeno-associated virus vector genomes are primarily responsible for stable liver transduction in vivo. J. Virol. **75:**6969–6976.
46. **Nathwani, A. C., A. Davidoff, H. Hanawa, J. F. Zhou, E. F. Vanin, and A. W. Nienhuis.** 2001. Factors influencing in vivo transduction by recombinant adeno-associated viral vectors expressing the human factor IX cDNA. Blood **97:**1258–1265.
47. **Qing, K., J. Hansen, K. A. Weigel-Kelley, M. Tan, S. Zhou, and A. Srivastava.** 2001. Adeno-associated virus type 2-mediated gene transfer: role of cellular FKBP52 protein in transgene expression. J. Virol. **75:**8968–8976.
48. **Qing, K., B. Khuntirat, C. Mah, D. M. Kube, X. S. Wang, S. Ponnazhagan, S. Zhou, V. J. Dwarki, M. C. Yoder, and A. Srivastava.** 1998. Adeno-associated virus type 2-mediated gene transfer: correlation of tyrosine phosphorylation of the cellular single-stranded D sequence-binding protein with transgene expression in human cells in vitro and murine tissues in vivo. J. Virol. **72:**1593–1599.
49. **Qing, K., W. Li, L. Zhong, M. Tan, J. Hansen, K. A. Weigel-Kelley, L. Chen, M. C. Yoder, and A. Srivastava.** 2003. Adeno-associated virus type 2-mediated gene transfer: role of cellular T-cell protein tyrosine phosphatase in transgene expression in established cell lines in vitro and transgenic mice in vivo. J. Virol. **77:**2741–2746.
50. **Qing, K., X. S. Wang, D. M. Kube, S. Ponnazhagan, A. Bajpai, and A. Srivastava.** 1997. Role of tyrosine phosphorylation of a cellular protein in adeno-associated virus 2-mediated transgene expression. Proc. Natl. Acad. Sci. USA **94:**10879–10884.
51. **Qiu, J., R. Nayak, and D. J. Pintel.** 2004. Alternative polyadenylation of adeno-associated virus type 5 RNA within an internal intron is governed by

both a downstream element within the intron 3′ splice acceptor and an element upstream of the P41 initiation site. J. Virol. **78:**83–93.

52. **Qiu, J., R. Nayak, G. E. Tullis, and D. J. Pintel.** 2002. Characterization of the transcription profile of adeno-associated virus type 5 reveals a number of unique features compared to previously characterized adeno-associated viruses. J. Virol. **76:**12435–12447.
53. **Qiu, J., and D. J. Pintel.** 2004. Alternative polyadenylation of adeno-associated virus type 5 RNA within an internal intron is governed by the distance between the promoter and the intron and is inhibited by U1 small nuclear RNP binding to the intervening donor. J. Biol. Chem. **279:**14889–14898.
54. **Riu, E., D. Grimm, Z. Huang, and M. A. Kay.** 2005. Increased maintenance and persistence of transgenes by excision of expression cassettes from plasmid sequences in vivo. Hum. Gene Ther. **16:**558–570.
55. **Rutledge, E. A., C. L. Halbert, and D. W. Russell.** 1998. Infectious clones and vectors derived from adeno-associated virus (AAV) serotypes other than AAV type 2. J. Virol. **72:**309–319.
56. **Samulski, R. J., A. Srivastava, K. I. Berns, and N. Muzyczka.** 1983. Rescue of adeno-associated virus from recombinant plasmids: gene correction within the terminal repeats of AAV. Cell **33:**135–143.
57. **Sanlioglu, S., D. Duan, and J. F. Engelhardt.** 1999. Two independent molecular pathways for recombinant adeno-associated virus genome conversion occur after UV-C and E4orf6 augmentation of transduction. Hum. Gene Ther. **10:**591–602.
58. **Sarkar, R., R. Tetreault, G. Gao, L. Wang, P. Bell, R. Chandler, J. M. Wilson, and H. H. Kazazian, Jr.** 2004. Total correction of hemophilia A mice with canine FVIII using an AAV 8 serotype. Blood **103:**1253–1260.
59. **Schmidt, M., H. Katano, I. Bossis, and J. A. Chiorini.** 2004. Cloning and characterization of a bovine adeno-associated virus. J. Virol. **78:**6509–6516.
60. **Smith, R. H., S. A. Afione, and R. M. Kotin.** 2002. Transposase-mediated construction of an integrated adeno-associated virus type 5 helper plasmid. BioTechniques **33:**204–206, 208, 210–211.
61. **Snyder, R. O., D. S. Im, T. Ni, X. Xiao, R. J. Samulski, and N. Muzyczka.** 1993. Features of the adeno-associated virus origin involved in substrate recognition by the viral Rep protein. J. Virol. **67:**6096–6104.
62. **Snyder, R. O., C. H. Miao, G. A. Patijn, S. K. Spratt, O. Danos, D. Nagy, A. M. Gown, B. Winther, L. Meuse, L. K. Cohen, A. R. Thompson, and M. A. Kay.** 1997. Persistent and therapeutic concentrations of human factor IX in mice after hepatic gene transfer of recombinant AAV vectors. Nat. Genet. **16:**270–276.
63. **Thomas, C. E., T. A. Storm, Z. Huang, and M. A. Kay.** 2004. Rapid uncoating of vector genomes is the key to efficient liver transduction with pseudotyped adeno-associated virus vectors. J. Virol. **78:**3110–3122.
64. **Wang, L., R. Calcedo, T. C. Nichols, D. A. Bellinger, A. Dillow, I. M. Verma, and J. M. Wilson.** 2005. Sustained correction of disease in naive and AAV2-pretreated hemophilia B dogs: AAV2/8-mediated, liver-directed gene therapy. Blood **105:**3079–3086.
65. **Wang, X. S., S. Ponnazhagan, and A. Srivastava.** 1996. Rescue and replication of adeno-associated virus type 2 as well as vector DNA sequences from recombinant plasmids containing deletions in the viral inverted terminal repeats: selective encapsidation of viral genomes in progeny virions. J. Virol. **70:**1668–1677.
66. **Wang, X. S., K. Qing, S. Ponnazhagan, and A. Srivastava.** 1997. Adeno-associated virus type 2 DNA replication in vivo: mutation analyses of the D sequence in viral inverted terminal repeats. J. Virol. **71:**3077–3082.
67. **Weger, S., A. Wistuba, D. Grimm, and J. A. Kleinschmidt.** 1997. Control of adeno-associated virus type 2 cap gene expression: relative influence of helper virus, terminal repeats, and Rep proteins. J. Virol. **71:**8437–8447.
68. **Xiao, W., N. Chirmule, S. C. Berta, B. McCullough, G. Gao, and J. M. Wilson.** 1999. Gene therapy vectors based on adeno-associated virus type 1. J. Virol. **73:**3994–4003.
69. **Xiao, X., W. Xiao, J. Li, and R. J. Samulski.** 1997. A novel 165-base-pair terminal repeat sequence is the sole *cis* requirement for the adeno-associated virus life cycle. J. Virol. **71:**941–948.
70. **Yan, Z., R. Zak, Y. Zhang, and J. F. Engelhardt.** 2005. Inverted terminal repeat sequences are important for intermolecular recombination and circularization of adeno-associated virus genomes. J. Virol. **79:**364–379.
71. **Yang, J., W. Zhou, Y. Zhang, T. Zidon, T. Ritchie, and J. F. Engelhardt.** 1999. Concatemerization of adeno-associated virus circular genomes occurs through intermolecular recombination. J. Virol. **73:**9468–9477.
72. **Yue, Y., and D. Duan.** 2003. Double strand interaction is the predominant pathway for intermolecular recombination of adeno-associated viral genomes. Virology **313:**1–7.
73. **Zentilin, L., A. Marcello, and M. Giacca.** 2001. Involvement of cellular double-stranded DNA break binding proteins in processing of the recombinant adeno-associated virus genome. J. Virol. **75:**12279–12287.